

Comparison Between Cycle-to-Cycle Variations in the Coefficient of Joy’s Law and Covariance of Rotation Residuals and Meridional Motions of Sunspot Groups

J. Javaraiah^{*} †

Bikaspura, BSK 5th Stage, Bengaluru-560 111, India

Accepted XXX. Received YYY; in original form ZZZ

ABSTRACT

The tilts of bipolar magnetic regions are believed to be caused by the action of Coriolis force on rising magnetic flux tubes. Here we analysed the combined Greenwich and Debrecen observatories sunspot-group data during the period 1874–2017 and the tilt angles of sunspot groups measured at Mt. Wilson Observatory during the period 1917–1986 and Debrecen Observatory during the period 1994–2013. We find that there exists about 8-solar cycle (Gleissberg cycle) trend in the long-term variation of the slope of Joy’s law (increase of tilt angle with latitude). There exists a reasonably significant correlation between the slope/coefficient of Joy’s law and the slope (namely, residual covariance) of the linear relationship between the rotation residuals and meridional motions of sunspot groups in the northern hemisphere and also in the southern hemisphere during Solar Cycles 16–21. We also find that there exists a good correlation between north–south difference (asymmetry) in the coefficient of Joy’s law and that in the residual covariance. We consider the residual covariance represents tentatively the coefficient of angular momentum transport. These results suggest that there exists a relationship between the surface/subsurface poleward/equatorward angular momentum transport and the Joy’s law. There is a suggestion of the strength of the Joy’s law depends on the strength of the poleward angular momentum transport.

Key words: Sun: activity – Sun: magnetic fields – Sun: rotation – (Sun): sunspots

1 INTRODUCTION

Ward (1965) analyzed Greenwich sunspot-group data during the period 1935–1944 and found a significant correlation between the angular and meridional velocities of sunspot groups and interpreted it as meridional flows transfer angular momentum toward equator. Later many scientists studied this correlation by using various data and methods (Sudar et al. 2014, 2017; Javaraiah 2021, and references therein). Theoretical models predicted this correlation as reflection of equatorial angular momentum transport caused by Reynolds stresses near the surface (e.g. Gilman 1986). Earlier, (Javaraiah 2021), we analysed the combined Greenwich and DPD sunspot-group data during the period 1874–2017 and studied solar cycle-to-cycle variation in the slope (namely, “residual covariance”) of the linear relationship between the rotation residuals and meridional motions of sunspot groups in the Sun’s whole-sphere. In the present analysis we analysed the same sunspot-group data and determined the residual covariance and its solar cycle-to-cycle modulations in northern and southern hemispheres.

The line joining the leading and following parts of an active region makes an angle to the parallel of the local latitude. This angle is referred to as tilt angle of the active region. Various dynamic characteristics of active regions seem to be depend on the tilt angles of

active regions (Howard 1991, 1996c). The average tilt angle of active regions increases with latitude (Hale et al. 1919). It is referred to as Joy’s law and has been studied extensively (for references see Gao 2023). Recently, (Javaraiah 2023), we analysed Mt. Wilson Observatory (MWOB) sunspot-group data during the period 1917–1986 and studied the solar cycle-to-cycle modulations in the coefficient of Joy’s law during Solar Cycles 15–21 in the whole-sphere and northern and southern hemispheres.

The tilts of bipolar magnetic regions are believed to be caused by the action of Coriolis force on rising magnetic flux tubes. Coriolis force may be responsible for Joy’s law and hence the latter could be related to the equatorward/poleward angular momentum transport. In the present analysis, in order to check whether there exists a relationship between the cycle-to-cycle variations in the Joy’s law and the poleward/equatorward angular momentum transport, we determined correlation between the cycle-to-cycle variations in the coefficients of Joy’s law and residual covariance during Solar Cycles 15–21 determined from the whole-sphere data and the northern and southern hemispheres’ data separately. We consider the residual covariance as the coefficient of angular momentum transport.

In the next section we describe the data and analysis. In Section 3 we describe the results and in Section 4 we present the conclusions and briefly discuss them.

^{*} E-mail: jajj55@yahoo.co.in; jj@iip.res.in

† Formerly worked in Indian Institute of Astrophysics, Bengaluru-560 034, India

2 DATA ANALYSIS

2.1 Determination of the "Residual Covariance" From Greenwich and DPD Sunspot-group Data

Earlier, [Javaraiah \(2021\)](#), we analysed the combined Greenwich Photoheliographic Results (GPR) and Debrecen Photoheliographic Data (DPD) of sunspot-group during 1874–2017. The solar sidereal angular velocity ω (in degree day⁻¹) was calculated as $\omega(\theta) = \frac{L_i - L_{i-1}}{t_i - t_{i-1}} + 14^\circ.18$, and the meridional velocity v_{mer} (in degree day⁻¹) of the sunspot group was calculated as $v_{mer}(\theta) = \frac{\lambda_i - \lambda_{i-1}}{t_i - t_{i-1}}$, where L_{i-1} and L_i are heliographic longitudes, and λ_{i-1} and λ_i are heliographic latitudes of a sunspot group measured at times t_{i-1} and t_i during the life time (disk passage) of the sunspot group, $\theta = \lambda_{i-1}$, and $14^\circ.18$ day⁻¹ is the Carrington rigid body rotation rate. These daily values in each year during 1874–2017 were binned into different 5° latitude intervals (0–5°), (5–10°),...,(35–40°) of the northern and southern hemispheres, and calculated the mean values of $\langle \bar{\omega} \rangle(\lambda)$ and $\langle \bar{v}_{mer} \rangle(\lambda)$ in each latitude interval in which the data were available, where λ is the middle value of a latitude interval (note that ‘-’ indicates mean over a latitude interval and ‘.’ indicates mean over time, a year). Using the $\langle \bar{\omega} \rangle(\lambda)$ of all the latitude intervals in all the years during the whole period 1874–2017 we obtained the grand differential rotation law, $\langle \bar{\omega} \rangle(\lambda) = (14.5 \pm 0.01) - (2.2 \pm 0.07) \sin^2 \lambda$ degree/day. For each latitude interval of a year we determined the residual rotation $\Delta \langle \bar{\omega}_{rot} \rangle(\lambda) = \langle \bar{\omega} \rangle(\lambda) - \xi(\lambda)$, where $\xi(\lambda)$ is the value of $\langle \bar{\omega} \rangle(\lambda)$ deduced from the differential rotation law. The $\Delta \langle \bar{\omega} \rangle(\lambda)$ degree/day was converted into $\Delta \langle \bar{v}_{rot} \rangle(\lambda)$ meter/second and the values of $\langle \bar{v}_{mer} \rangle(\lambda)$ was also converted to the unit meter/second. The values of $\Delta \langle \bar{v}_{rot} \rangle(\lambda)$ and $\langle \bar{v}_{mer} \rangle(\lambda)$ of all the years of a solar cycle were fitted to the following linear equation:

$$\langle \bar{v}_{mer} \rangle = D \Delta \langle \bar{v}_{rot} \rangle + C. \quad (1)$$

From this equation we have the following possibilities: When $\langle \bar{v}_{rot} \rangle$ is a positive value, a positive/negative D mostly produces a positive/negative $\langle \bar{v}_{mer} \rangle$ (poleward/equatorward motion). Obviously, it is opposite when $\langle \bar{v}_{rot} \rangle$ is a negative value. That is, the slope D (namely, residual covariance) is a dimensionless quantity, its sign indicates the direction of angular momentum transport. Therefore, we consider that the slope D represents tentatively the coefficient of poleward/equatorward angular momentum transport. A negative/positive value of D indicates equatorward/poleward angular momentum transport (also see [Sudar et al. 2014, 2017](#)).

Note that the correlation between the two horizontal forces (the ‘covariance’), the rotational and meridional motions, may represent angular momentum transport toward equator by Reynolds stresses that is believed to be responsible for solar differential rotation. Numerical simulations by [Brun \(2004\)](#) suggest that the Maxwell stresses related to the magnetic fields tend to oppose the Reynolds stresses causing poleward angular momentum transport. It may be also worth to note that sunspots exhibit both equatorward and poleward meridional motions ([Javaraiah & Ulrich 2006](#)).

The data reduction was carried out with all the necessary precautions that were taken care in [Javaraiah \(2021\)](#). In that paper we have studied the solar cycle-to-cycle modulation in D determined from the whole-sphere’s sunspot-group data during Solar Cycles 12–24 (note that in the case of Solar Cycle 24 the data were incomplete). Here the northern and southern hemispheres’ data are separately fitted to equation 1 and determined the northern and southern hemispheres’ values of D . However, we find that there exists no significant correlation between the amplitude (R_M) of a solar cycle and the corresponding slope D of the whole sphere as well as that of any hemisphere.

2.2 Recovering Joy’s law From MWOB Sunspot-group Data

Recently, [Javaraiah \(2023\)](#), we analysed the daily sunspot-group data measured in MWOB during the period 1917–1986. We binned the daily sunspot-group tilt angle (γ) data to the different 5°-latitude bins (absolute) 0–5°, 5–10°,... ,25–30°, 30–35°. First the whole-sphere’s data were analysed and then the northern and southern hemispheres’ data were analysed separately. We determined the average values of tilt angle ($\langle \bar{\gamma} \rangle$) in each latitude bin during a solar cycle and they were fitted to the following linear equation (here ‘.’ indicates mean over a solar cycle):

$$\langle \bar{\gamma} \rangle = m|\lambda| + c, \quad (2)$$

where $|\lambda|$ is the absolute middle value of a latitude interval and the slope m represents the coefficient of Joy’s law. A positive value of m implies leading group closer to the equator than following group. We studied solar cycle-to-cycle modulations in m determined from the whole-sphere data and also that determined separately from the northern and southern hemispheres’ data in each of Solar Cycles 15–21 (note that the data of first 4 years of Solar Cycle 15 and the last year of Solar Cycle 21 are missing). Only the southern hemisphere’s m of a solar cycle was found to be reasonably well correlate to the amplitude (R_M) of the solar cycle.

2.3 Determination of Correlation Between m and D

Here we have used the values of m determined in [Javaraiah \(2023\)](#) for all the three cases: whole-sphere, northern hemisphere, and southern hemisphere. We have used the values of the whole sphere’s D that are taken from Table 2 of [Javaraiah \(2021\)](#) and the corresponding hemispheres’ values that are determined in the present analysis. We determined correlation between solar cycle-to-cycle variations in m and D during Solar Cycles 15–21 for aforementioned all the three cases. Except in the case of equation 1, in each of the remaining linear regression analyses presented in this article the uncertainties in both abscissa and ordinate are taken care in the calculation of the linear-least-square fit. For this we used the Interactive Digital Library (IDL) software FITEXY.PRO, which is downloaded from the website idlastro.gsfc.nasa.gov/ftp/pro/math/. In the case of equation 1, when we have used the uncertainties in $\Delta \langle \bar{v}_{rot} \rangle$ and $\langle \bar{v}_{mer} \rangle$ the corresponding least-square best-fits were found not good.

In [Javaraiah \(2023\)](#) we studied the variations in m determined from both the tilt-angle data and the area-weighted tilt-angle data (the corresponding values were given in Tables 3–5 of that paper). However, here we have used only the values of m that were determined from the tilt-angle data. This is because no reasonable correlation between m and D was found when we have used the values of m derived from the area weighted tilt-angle data, in all the three cases: whole sphere, northern hemisphere, and southern hemisphere.

2.4 Recovering Joy’s law From DPD Sunspot-group Data

Recently, [Gao \(2023\)](#) has analysed the DPD sunspot-group tilt-angle data during the period 1994–2013 and has found that the cyclical behaviors of the tilt angles during Solar Cycle 23 are different from those of Solar Cycles 21 and 22. Here we also analysed the same data (downloaded from <http://fenyi.solarobs.csfk.mta.hu/test/tiltangle/dpd/>) and determined the values of m (the slope of equation 2) for Solar Cycle 21–23 for all the three cases: whole sphere, northern hemisphere, and southern hemisphere. For the detailed description of the DPD data can be found in ([Baranyi 2015](#); [Baranyi et al. 2016](#); [Győri et al. 2017](#)). We analysed the data of the

Table 1. Values of the intercept (C) and slope (D), and the corresponding standard deviations (σ_C) and (σ_D) of the linear-relationship between $\langle v_{mer}(\theta) \rangle$ and $\Delta \langle v_{rot}(\theta) \rangle$ (equation 1) determined from the northern and southern hemisphere's sunspot-group data during each solar cycle (^a indicates incomplete data) and during the whole period 1874–2017. The corresponding values of the correlation coefficient (r), Student's t (τ) and probability (P) are given. The n represents the number of data points in a solar cycle.

Cycle	Time	C	σ_C	D	σ_D	r	τ	P	n
Derived from northern hemisphere's data									
12	1878–1889	2.122	1.169	0.028	0.036	0.12	0.79	0.784	48
13	1890–1901	-2.346	1.195	-0.030	0.035	-0.12	0.85	0.801	51
14	1902–1912	0.079	1.374	0.027	0.043	0.10	0.62	0.731	44
15	1913–1922	-0.992	1.083	-0.044	0.044	-0.15	1.00	0.839	47
16	1923–1932	-0.318	0.903	-0.024	0.027	-0.12	0.89	0.811	52
17	1933–1943	-1.643	0.987	-0.061	0.036	-0.22	1.68	0.951	56
18	1944–1953	-2.517	0.909	-0.092	0.041	-0.31	2.28	0.987	52
19	1954–1963	-0.606	0.929	0.005	0.033	0.02	0.15	0.559	63
20	1964–1975	1.155	0.779	-0.089	0.029	-0.35	3.02	0.998	69
21	1976–1985	-0.236	1.156	0.090	0.053	0.23	1.71	0.953	56
22	1986–1995	1.641	0.942	-0.057	0.039	-0.20	1.45	0.924	54
23	1996–2007	2.280	0.973	0.017	0.040	0.05	0.43	0.665	65
24 ^a	2008–2017	-1.839	1.374	-0.096	0.057	-0.25	1.69	0.951	44
1874–2017		-0.117	0.283	-0.020	0.010	-0.07	2.00	0.977	711
Derived from southern hemisphere's data									
12	1878–1889	-0.355	1.079	-0.088	0.038	-0.31	2.29	0.987	51
13	1890–1901	1.281	1.190	0.010	0.046	0.03	0.21	0.585	54
14	1902–1912	0.068	1.080	0.032	0.038	0.13	0.85	0.800	41
15	1913–1922	-1.363	1.026	-0.127	0.044	-0.41	2.90	0.997	44
16	1923–1932	-0.444	1.163	-0.028	0.045	-0.09	0.61	0.729	49
17	1933–1943	0.527	0.909	0.076	0.036	0.28	2.11	0.980	53
18	1944–1953	0.242	1.081	-0.094	0.040	-0.29	2.32	0.988	59
19	1954–1963	1.039	1.008	-0.096	0.032	-0.38	2.98	0.998	54
20	1964–1975	0.842	1.077	-0.007	0.036	-0.03	0.20	0.581	56
21	1976–1985	-0.214	1.091	-0.022	0.039	-0.07	0.56	0.712	61
22	1986–1995	0.213	1.096	-0.041	0.045	-0.12	0.92	0.818	57
23	1996–2007	0.701	0.917	-0.054	0.045	-0.15	1.19	0.880	66
24 ^a	2008–2017	3.145	1.221	0.019	0.061	0.05	0.31	0.620	42
1874–2017		0.395	0.295	-0.033	0.011	-0.11	2.98	0.998	699

tilt angles correspond to the whole-spot areas of sunspot groups and also the tilt angles correspond to only the umbrae areas of sunspot groups. The latter is similar to the MWOB tilt-angle data. We have used the tilt angles of sunspot groups whose leading and following parts were separated by $> 2.5^\circ$. This is because the data correspond to the separations $\leq 2.5^\circ$ contain large number of unipolar sunspot groups (Baranyi 2015). We calculated the polarity separation (Δs) by using the formula given by Jiao et al. (2021): $\cos(\Delta s) = \sin(\lambda_f) \sin(\lambda_l) + \cos(\lambda_f) \cos(\lambda_l) \times \cos(\phi_f - \phi_l)$, where λ_f and λ_l are the latitudes of the following and leading polarities, respectively, and ϕ_f and ϕ_l are the corresponding longitudes. The sign convention of the DPD tilt angles are the same as those of MWOB, i.e. a positive value of m implies leading group closer to equator than following group, in both the northern and southern hemispheres. We have excluded the data correspond to the central meridian distance (CMD) $> 60^\circ$. In the case of DPD data we found a reasonable amount of the data also in the latitude interval $35 - 40^\circ$ and hence we have used this interval data also in the determination of the values of m in all the three cases: whole sphere, northern hemisphere, and southern hemisphere, whereas in this latitude interval the MWOB data were found to be absent or inadequate in all the three cases and hence they were not considered.

3 RESULTS

Fig. 1 shows the relationship between meridional velocity and residual rotation rate determined by the combined data of sunspot groups in northern and southern hemispheres during the whole period 1874–2017. In Table 1 we have given the values of the coefficients C and D , and their uncertainties (values of standard deviation σ), of equation 1, i.e. the linear relationship between $\langle v_{mer}(\theta) \rangle$ and $\Delta \langle v_{rot}(\theta) \rangle$ derived here from the northern and southern hemispheres' sunspot group data during each solar cycle and also from

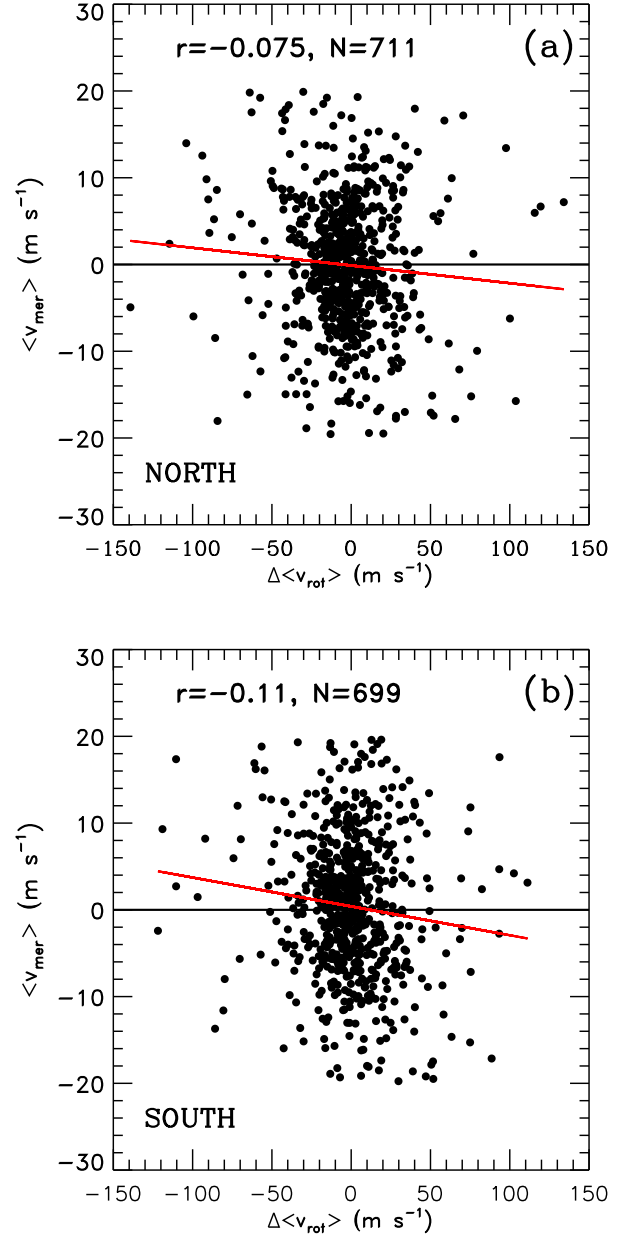


Figure 1. Scatter plot of meridional velocity ($\langle v_{mer}(\theta) \rangle$) from -20 to $+20$ m s^{-1} versus residual rotation rate ($\Delta \langle v_{rot}(\theta) \rangle \approx -140$ to $+140$ m s^{-1}) determined by the combined data of sunspot groups (a) in northern hemisphere and (b) in southern hemisphere during the whole period 1874–2017. The correlation coefficient (r) and number of data points N , is also shown. Positive values of meridional velocity indicate poleward motions and negative values indicate equatorward motions, both hemispheres. The continuous line (red) represents the linear best-fit.

the data during the whole period 1874–2017. In the same table we have also given the values of the correlation coefficient (r), Student's t (τ) and the corresponding probability (P), minimum epoch of solar cycle, and number of data points. These values indicate that the relationship between the meridional velocity and residual rotation rate is reasonably good in some solar cycles and is not good in some other solar cycles. The value of D determined from the whole period

Table 2. Values of the intercept (c) and the slope (m), and the corresponding standard deviations σ_c and σ_m , respectively, determined from the linear-least-square fits of the DPD tilt angle data of Solar Cycles (SC) 21–23 to the equation 2. The values of correlation coefficient (r), χ^2 and the corresponding probability (P), the ratio m/σ_m , and the rms (root-mean-square deviation) are also given.

SC	c	σ_c	m	σ_m	r	χ^2	P	m/σ_m	rms
From sunspot groups with whole-spot areas									
Whole sphere									
21	1.88	0.80	0.26	0.04	0.79	8.65	0.19	6.50	1.94
22	0.58	0.98	0.36	0.05	0.97	4.73	0.58	7.20	1.05
23	1.50	0.89	0.36	0.04	0.97	4.03	0.67	9.00	1.13
Northern hemisphere									
21	2.40	0.93	0.25	0.04	0.79	9.12	0.17	6.25	1.86
22	-0.73	1.31	0.42	0.06	0.93	10.23	0.12	7.00	1.89
23	1.66	1.07	0.36	0.05	0.75	10.58	0.10	7.20	2.85
Southern hemisphere									
21	1.06	1.15	0.29	0.05	0.62	10.60	0.10	5.80	3.05
22	1.30	1.07	0.34	0.05	0.91	7.54	0.27	6.80	1.77
23	0.82	1.11	0.41	0.05	0.97	4.10	0.66	8.20	1.09
From sunspot groups with only umbrae areas									
Whole sphere									
21	2.04	0.89	0.28	0.04	0.96	1.63	0.95	7.00	0.93
22	-1.72	1.18	0.48	0.05	0.99	3.66	0.72	9.60	0.92
23	0.20	0.99	0.39	0.04	0.90	8.83	0.18	9.75	1.98
Northern hemisphere									
21	1.98	1.10	0.31	0.05	0.87	7.71	0.26	6.20	1.84
22	-2.47	1.52	0.53	0.07	0.88	6.39	0.38	7.57	3.04
23	0.16	1.29	0.42	0.06	0.68	13.88	0.03	7.00	3.93
Southern hemisphere									
21	1.75	1.15	0.27	0.05	0.93	2.63	0.85	5.40	1.20
22	-1.17	1.26	0.44	0.06	0.94	8.51	0.20	7.33	1.92
23	-0.11	1.11	0.39	0.05	0.97	4.54	0.60	7.80	1.02

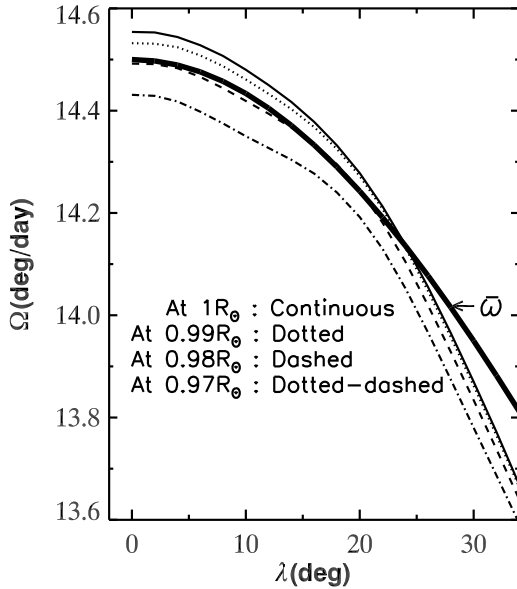


Figure 2. Latitude (λ) variations of the Sun's mean (over the whole period 1995–2009) internal rotation rate (Ω) at $0.97R_\odot$, $0.98R_\odot$, $0.99R_\odot$, and $1R_\odot$ (where R_\odot is the radius of the Sun) derived by H. M. Antia from GONG data. The thick-continuous curve represents the latitude variation of the mean angular velocity ($\bar{\omega}$) obtained by using the grand differential rotation law derived from the sunspot-group data (cf. Sec. 2).

sunspot group data is statistically significant on 2σ and 3σ levels in the northern and southern hemispheres, respectively. There exists a north-south difference in the slope (D) but it is small (only at 1σ -level). Note that the values of C , D , etc. derived from the whole sphere sunspot-group data were given in Table 2 of Javaraiah (2021).

Heliosismic studies indicated that a net longitude-

averaged meridional flow converging onto the active latitudes (Zhao & Kosovichev 2004; Hanasoge 2022, and references therein). Combined with the known torsional oscillation pattern this yields a *positive* (i.e. poleward) net residual correlation in plasma motions in the activity belt, opposite to that is found here (overall D has negative sign). However, the measured meridional velocities have considerably large uncertainties. Already mentioned above sunspots exhibit both equatorward and poleward meridional motions (Javaraiah & Ulrich 2006). Generally, the studies based on magnetic feature tracking (e.g Snodgrass & Dailey 1996) suggest equatorward angular momentum transport.

It has been argued that motions of magnetic tracers, such as sunspots, are no tracers of plasma motion. Instead, their motion is determined by a complex interplay of magnetic forces and geometrical projection factors like the asymmetry of emerging flux loops (Petrovay & Christensen 2010). Difficult to disprove this argument, and it is beyond the scope of the present analysis. On the other hand, although sunspot motions may not be fully proxy of surface plasma motions, to some extent proxy of the subsurface plasma motions (Howard 1996a). Fig. 2 shows latitude variations of the Sun's mean (over the whole period 1995–2009) internal plasma rotation rates at $0.97R_\odot$, $0.98R_\odot$, $0.99R_\odot$, and $1R_\odot$ (where R_\odot is the radius of the Sun) derived by H. M. Antia from the Global Oscillation Network Group (GONG) data. In the same figure we have also shown the latitude variation of the angular velocity ($\bar{\omega}$) obtained by using the grand differential rotation law derived above from the sunspot-group data (see Sec. 2). As we can see in this figure the differential rotational profile determined from the sunspot-group data closely match with the corresponding profile of the internal rotation rate at $0.98R_\odot$ ($r = 0.999$), at least up to about 25° latitude (also see Javaraiah & Komm 1999; Javaraiah 2013). Therefore, one can believe that the motions of sunspots are at least partially the tracers of plasma motions. (In Javaraiah (2021) and here large restrictions were applied to the data. Consequently, we have obtained slightly more flat $\bar{\omega}(\lambda)$ profile.)

Area-weighted heliographic positions of sunspot groups seem to be to a large extent increase uncertainties in the measured velocities (e.g. Kutsenko & Abramenko 2021). In the case of Greenwich sunspot data that we have used the positions of sunspot groups are geometrical (not the area-weighted) positions of centers of groups. The midpoints of sunspot groups measured on photographic plates were taken as positions of the groups (Poljančić et al. 2011).

Hereafter the D and m that are derived from the data of the whole sphere, northern hemisphere, and southern hemisphere are indicated with suffixes W, N, and S, respectively. In the case of the whole period, the north-south difference (north-south asymmetry), $D_{asym} = D_N - D_S$, is statistically significant. That is, the uncertainty $\sigma_{asym} = \sqrt{(\sigma_N^2/n_N + \sigma_S^2/n_S)}$ in D_{asym} is small ($D_{asym} = 0.013$ is about three times larger than its uncertainty 0.004), where σ_N and σ_S are the values of the uncertainties (σ values) in D_N and D_S , respectively, and n_N and n_S are the number of velocity values (values of n) gone in the determinations of D_N and D_S , respectively (see Table 1). The values of m_N and m_S determined from the MWOB whole period 1917–1986 tilt-angle data were given in Table 2 of Javaraiah (2023). The corresponding value of the north-south asymmetry, $m_{asym} = m_N - m_S$, is statistically significant on 95% confidence level, i.e. $m_{asym} = 0.05$ is about two times larger than the value 0.024 of its uncertainty (the value of m_{asym} derived from the area-weighted tilt angle data is found to be about five times larger than its uncertainty.)

In Table 2 we have given the values of the parameters of the

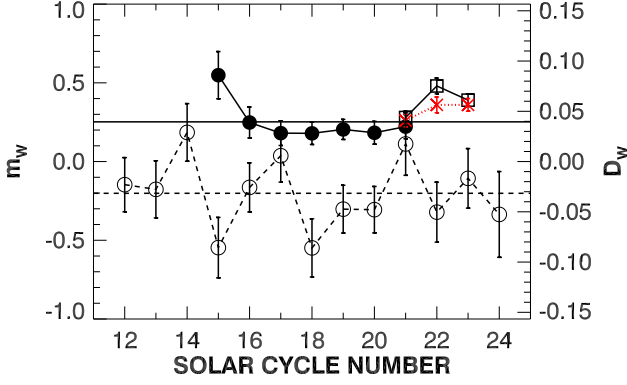


Figure 3. Solar cycle-to-cycle variations in the coefficient of Joy's law (m_W , filled circle-continuous curve) derived from the MWOB whole-sphere sunspot-group data during Solar Cycles 15–21 and the residual covariance (D_W , open circle-dashed curve) derived from the combined GPR and DPD whole-sphere's sunspot-group data during Solar Cycles 12–24 (the MWOB data of Solar Cycle 15 and the DPD data of Solar Cycle 24 are incomplete). The mean values of the m_W and D_W are shown by horizontal continuous and dashed lines, respectively. The values of m_W (given in Table 2) determined from the DPD tilt-angle data corresponding to the whole-spot areas (red cross-dotted curve) and that corresponding to the umbrae areas (square-continuous curve) of sunspot groups are also shown.

Joy's laws, i.e. the linear relationships of tilt angles and the latitudes of sunspot groups, determined from the DPD tilt-angle data corresponding to the whole-spot areas and only the umbrae areas of the sunspot groups in the whole sphere, and the northern and the southern hemispheres during each of the complete Solar Cycles 21–23. In most of the cases the linear relationship is reasonably good, i.e. the correlation is statistically significant, χ^2 is insignificant (the 95% significant value of χ^2 is 14.067 for 7 degrees of freedom), and the ratio of the slope to its uncertainty is reasonably high. In each of the three cases: whole sphere, northern hemisphere, and southern hemispheres, the pattern of the slope of Joy's law during Solar Cycles 21–23 determined from the DPD tilt-angle data is slightly different from that obtained by Jiao et al. (2021) using the DPD area-weighted tilt angles and forcing the linear function pass through the origin.

Fig. 3 shows the solar cycle-to-cycle variations in m_W derived from the MWOB whole-sphere's sunspot-group data during Solar Cycles 15–21 (the values are taken from Table 3 of Javaraiah 2023) and D_W (the values are taken from Table 2 of Javaraiah 2021) derived from the combined GPR and DPD whole-sphere's sunspot-group data during Solar Cycles 12–24 (note that the MWOB data of Solar Cycle 15 and the DPD data of Solar Cycle 24 are incomplete). In the same figure we have also shown the values of m determined here from the DPD tilt-angle data of Solar Cycles 21–23, for both the cases of whole-spot areas and only umbrae areas of sunspot groups. As we can see in this figure only the value of m_W of the incomplete Solar Cycle 15 significantly differs (large) the corresponding over all cycles' mean value (the mean value of m_W is calculated from the MWOB data only). The m_W is almost constant during Solar Cycles 16–21. The values of m_W (given in Table 2 above) determined from the DPD data of tilt angles corresponding to both the whole-spot areas and only umbrae areas of sunspot groups are slightly larger than the mean value. In Solar Cycles 14, 17, and 21, the values of D_W are statistically significant and have a positive

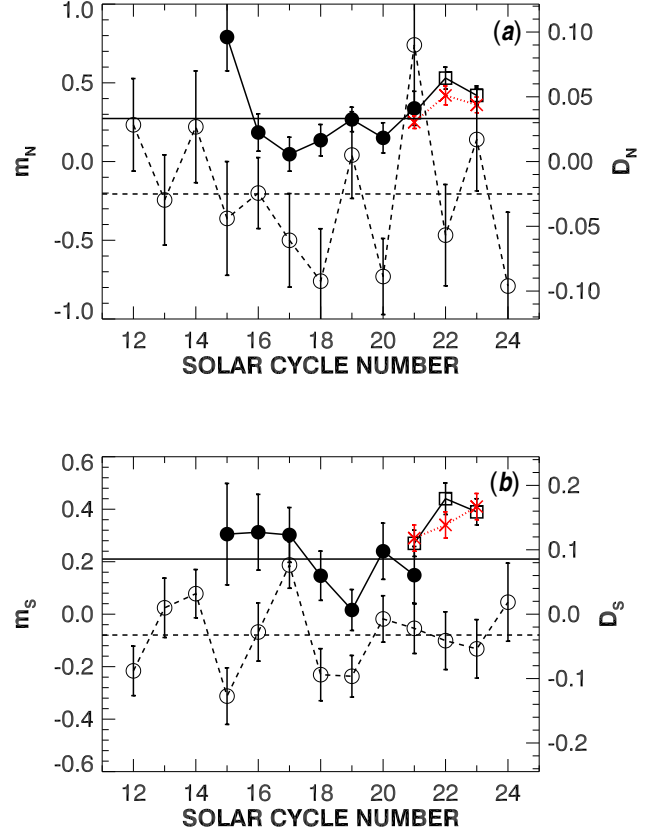


Figure 4. Solar cycle-to-cycle variations in the coefficients of Joy's law (m_N and m_S , filled circle-continuous curves) determined from the MWOB sunspot-group data during Solar Cycles 15–21 and the residual covariance (D_N and D_S , open circle-dashed curves) determined from the GPR and DPD sunspot-group data during Solar Cycles 12–24, in (a) northern and (b) southern hemispheres. The mean values of the m_N and m_S are shown by horizontal continuous lines, and the mean values of the D_N and D_S are shown by horizontal dashed lines. The values of m_N and m_S (given in Table 2) determined from the DPD tilt-angle data corresponding to the whole-spot areas (red cross-dotted curve) and that corresponding to the umbrae areas (square-continuous curve) of sunspot groups are also shown.

sign, whereas the corresponding values in Solar Cycles 15 and 18 are significant, but have a negative sign. It seems there exist 3–5 solar-cycle variations in D_W . Obviously, there exists no significant correlation/anticorrelation between m_W and D_W during Solar Cycles 15–21 ($r = -0.44$ only). In the case of Solar Cycles 21–23 the DPD data indicate an anti-correlation between m_W and D_W . The overall cycles' mean m_W is positive because in a large number of solar cycles m_W is positive, i.e. the leading portions of a large number of the sunspot groups closer to the equator than their respective following portions, in consistent with Joy's law. The overall cycles' mean D_W is negative means that in a large number of solar cycles the angular momentum transport is mostly toward equator.

Figs. 4a and 4b show the solar cycle-to-cycle variations in the coefficients of Joy's law (the values are taken from Tables 4 and 5 of Javaraiah 2023) and of the coefficients of equatorward/poleward angular momentum transport in the northern and southern hemispheres (values given in Table 1 above), respectively. As we can see in this figure the patterns of the variations in the coefficients m_N and m_S

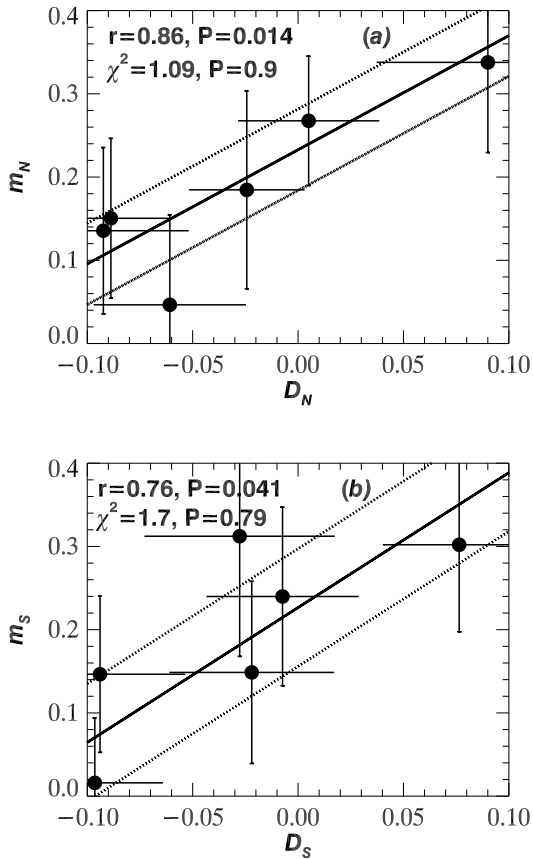


Figure 5. Scatter plots of residual covariance (D_N and D_S) versus the coefficient of Joy’s law (m_N and m_S) derived from (a) the northern hemisphere and (b) the southern hemisphere sunspot-group data during Solar Cycles 16–21. The *continuous line* represents the best-fit linear relation and the *dotted lines* are drawn at one-rms (*root-mean-square deviation*) levels. The value of correlation coefficient (r) and χ^2 and the values of the corresponding probabilities are also shown.

of Joy’s law determined from the MWOB data in the northern and southern hemispheres are considerably different. The patterns of the variations in the slopes D_N and D_S , i.e. the coefficients of the angular momentum transport in the northern and southern hemispheres, respectively, are also considerably different. The variation of m_N is in a large extent the same as that of the m_W shown in Fig. 3, but it looks to be correlate with the variation in D_N during Solar Cycles 16–21. The variation of m_S also looks to be correlate with D_S during Solar Cycles 16–21. However, both m_N and m_S (values given in Table 2 above) determined from the DPD tilt-angle data look to be slightly anti-correlate with the corresponding D_N and D_S during Solar Cycles 21–23. Both m_N and m_S have positive values in most solar cycles (consistent with Joy’s law), whereas both D_N and D_S have negative values in many solar cycles (equatorward angular momentum transport). The long-term trends of the variations in m_N and m_S (also in m_w , see Fig. 3) of MWOB and DPD data together suggest the existence of a long-term (around 8-solar cycle) cycle (Gleissberg cycle) in these parameters.

Since the first four years’ MWOB data of Solar Cycle 15 are missing, the corresponding values of $\langle \bar{\gamma} \rangle$ are not well determined and hence the slope of this solar cycle might be also not well determined. Hence, we calculated the correlation between the coefficients

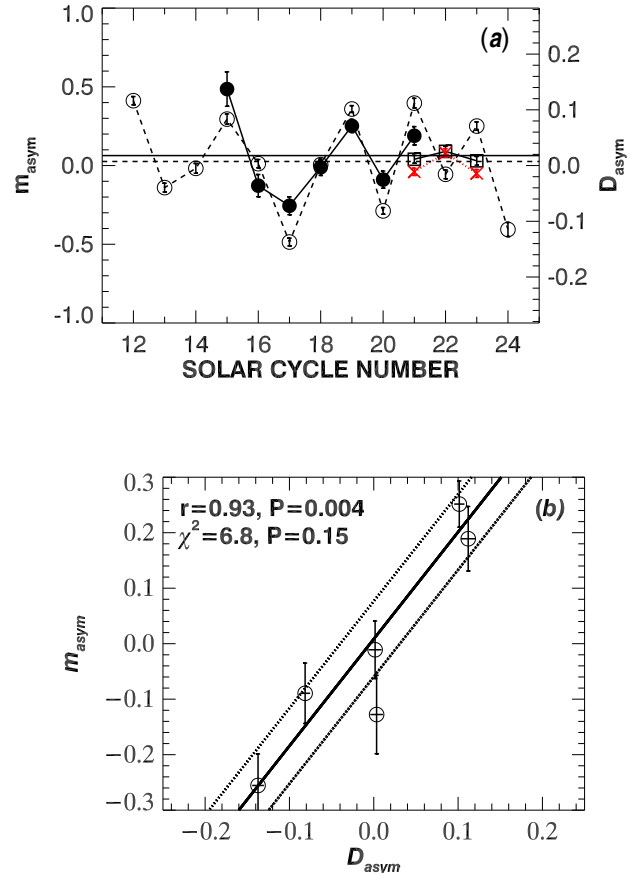


Figure 6. (a) Solar cycle-to-cycle variations in north–south difference (north–south asymmetry) in the coefficients of Joy’s law (m_{asym} : $m_N - m_S$, *filled circle-continuous curve*) determined from the MWOB sunspot group data during Solar Cycles 15–21 and of the north–south asymmetry in residual covariance (D_{asym} : $D_N - D_S$, *open circle-dashed curve*) derived from the combined GPR and DPD sunspot-group data during Solar Cycles 12–24, in the northern and southern hemispheres. The horizontal *continuous* and *dashed lines* are drawn at the mean values of m_{asym} and D_{asym} , respectively (note that the MWOB data of Solar Cycle 15 and the DPD data of Solar Cycle 24 are incomplete). The values of m_{asym} determined from the DPD tilt angles corresponding to the whole-spot areas (*red cross-dotted curve*) and that corresponding to the umbrae areas (*square-continuous curve*) of sunspot groups are also shown. (b) Scatter plot of D_{asym} versus m_{asym} during Solar Cycles 16–21. The *continuous line* represents the best fit linear relation and the horizontal *dotted lines* are drawn at one-rms levels. The values of correlation coefficient (r) and χ^2 and the corresponding probabilities are also shown.

of Joy’s law and residual covariance with and without including the data points of this solar cycle. In fact, when they were included the correlation was found to be very low. Moreover, the data points of the m_N and m_S of Solar Cycles 21–23 determined from the DPD tilt-angle data were not considered here and not included in the determination of correlation. This is because as we have already seen in Fig. 4 above, their behavior is different and seem to be anti-correlate with the corresponding D_N and D_S , respectively. Fig. 5 shows the correlation between the coefficients of Joy’s law and angular momentum transport in the northern and southern hemispheres during Solar Cycles 16–21. The correlation is highly statistically significant (more than 95% confidence level) in the northern hemisphere, and is about 95% confidence level in the southern hemisphere. We

obtained the following relations:

$$m_N = (1.37 \pm 0.82)D_N + 0.22 \pm 0.05, \text{ and} \quad (3)$$

$$m_S = (1.62 \pm 0.84)D_S + 0.23 \pm 0.05. \quad (4)$$

The values of χ^2 of the corresponding least-square best fits are small (statistically insignificant). The relationship (equation 3) in the northern hemisphere is slightly more accurately determined than that (equation 4) in the southern hemisphere (see Fig. 5). There is a suggestion that the variations of m_S with D_S are steeper than the variations of m_N with D_N . Overall, we can conclude that there exists a reasonably significant linear relationship between the coefficients of Joy's law and angular momentum transport in both the hemispheres during Solar Cycles 16–21. There exists no significant correlation between m_W and D_W . But there exists a reasonable correlation between the corresponding parameters of an hemisphere. This conveys that it is necessary and important to determine Joy's law and residual covariance and their relationship from the hemispheres' data separately.

Fig. 6a shows the solar cycle-to-cycle variation in the north–south difference, i.e. north–south asymmetry (m_{asym} : $m_N - m_S$), in the coefficients of Joy's law determined from the MWOB sunspot-group data during Solar Cycles 15–21, and the north–south asymmetry in residual covariance (D_{asym} : $D_N - D_S$) determined from the combined GPR and DPD sunspot-group data during Solar Cycles 12–24. The variation in m_{asym} determined from the DPD tilt-angle data during Solar Cycles 21–23 is also shown. As can be seen in this figure the cycle-to-cycle variations of the m_{asym} and D_{asym} are closely resemble each other during Solar Cycle 15–21, in such way that one can think that the behavior of m_{asym} before Solar Cycle 15 and after Solar Cycle 21 might be also similar as that of D_{asym} . But it seems not, i.e. the m_{asym} determined from the DPD tilt-angle data is not significantly different from zero during Solar Cycles 21–23 and seems to be to some extent anticorrelate to the corresponding D_{asym} . We calculated the correlation between the m_{asym} and D_{asym} with and without the data points of Solar Cycle 15 (the values of m_{asym} determined from the DPD data are not considered). With including the data points of Solar Cycle 15 we obtained $r = 0.84$ and without including these data points we obtained $r = 0.92$, both these are statistically significant on more than 95% confidence level. Fig. 6b shows the correlation between the D_{asym} and m_{asym} during Solar Cycles 16–21. We obtained the following linear relationship between the m_{asym} (derived from the MWOB data) and D_{asym} (derived from the GPR and DPD data) during Solar Cycles 16–21:

$$m_{\text{asym}} = (1.93 \pm 0.25)D_{\text{asym}} + 0.008 \pm 0.022. \quad (5)$$

The corresponding least-square best fit of this equation is very good, i.e. the value of the slope is about 7.7 times larger than the corresponding standard deviation and χ^2 is reasonably small (<95% significant level). In addition, value of the intercept is negligibly small, suggesting that there exists one-to-one correspondence between m_{asym} and D_{asym} .

In Figs. 4 and 5 there is also a suggestion of weak and strong Joy's laws largely associated with equatorward and poleward angular momentum transport, respectively, largely implying that the strength of the Joy's law depends on the strength of the poleward angular momentum transport. Overall, the results above, indicate that there exists a role of surface/subsurface poleward/equatorward angular momentum transport in the Joy's law of tilt angles of bipolar active regions (sunspot groups). Anti-Joy regions (those with the follower portion closer to the equator than the leading portion) may be mostly

related to the equatorward angular momentum transport (return flow in relatively deeper layers).

4 DISCUSSION AND CONCLUSIONS

Coriolis force may be responsible for Joy's law and hence the latter may be related to the equatorward/poleward angular momentum transport. Here we find that there exists around 8-solar cycle (Gleissberg cycle) trend in the long-term variation of the slope of Joy's law (increase of tilt angle with latitude). There exists a reasonably significant correlation between the solar cycle modulations in the coefficients of Joy's law and residual covariance determined from the northern and southern hemispheres' sunspot-group data during Solar Cycles 16–21. There exists also a good correlation between the north–south differences of these parameters. We consider the residual covariance D tentatively represents the coefficient of angular momentum transport. Overall these results indicate that there exists a role of surface/subsurface poleward/equatorward angular momentum transport (latitude dependent Reynolds stress) in the Joy's law of tilt angles of bipolar active regions. That is, there is a suggestion of the strength of the Joy's law depends on the strength of the poleward angular momentum transport.

The existence of a relationship between the tilt angles of active regions and the rotation rates of the active regions have been found. Howard (1996c) found that sunspot groups with the tilt angles near the average value or 0° , rotate significantly faster ($\approx 1\%$ between tilt angles of 0° and 45°) than do groups having tilt angles far from this value. There is a latitude dependence of this effect that follows Joy's law (Howard 1996b). However, in the present analysis we find no significant correlation between the mean residual rotation rate or the mean meridional velocity of the sunspot groups of a solar cycle and the coefficient of Joy's law of the solar cycle. The latter is found to be to some extent correlate ($r = 0.78$) with magnitude of the coefficient of differential rotation (magnitude of the latitude gradient of rotation) derived from sunspot group data in the northern hemisphere only (not in the southern hemisphere), suggesting that in the northern hemisphere an increase in the strength of the Joy's law to some extent associated with an increase in the strength of differential rotation. The aforementioned result that the existence of a reasonable correlation between the residual covariance (coefficient of angular momentum transport) and coefficient of Joy's law seems to be consistent with the conclusions of the models that invoke the effect of Coriolis force for cause of tilt angles of bipolar magnetic regions and Joy's law (e.g. D'Silva & Choudhuri 1993; Fisher et al. 1995).

Earlier, (Javaraiah 2023), we found that there exists a significant anti-correlation between m_S derived from the MWOB tilt-angle data and the amplitude (R_M) of a solar cycle and no a significant correlation exists between m_N and R_M . We found the m_{asym} of a solar cycle determined from the area-weighted tilt angles is significantly correlating with the amplitude (R_M) of the solar cycle and in the case of the tilt angles (not area-weighted), the correlation between m_{asym} and R_M was found to be statistically insignificant. It should be noted here that in the present analysis all the results are based on the tilt-angle data (no significant result is found from the area-weighted tilt-angle data). There exists no significant correlation between R_M and residual covariance in all the three cases: whole sphere, northern hemisphere, and southern hemisphere. Therefore, the effect of evolution of sunspot groups is less or absent in the present results.

Since here we find in both the hemispheres the coefficient of Joy's law is correlating to the residual covariance, hence we can conclude

that angular momentum transport has an important role in the mechanism behind the Joy's law. The strength of the Joy's law seems to be depending on the strength of the poleward angular momentum transport. However, further studies are necessary to find out the significant implications of the present results and their connection to the cycle-to-cycle modulation in the amplitudes of solar cycles.

Earlier no correlation was found between the slope of Joy's law of a solar cycle determined from the tilt angles of sunspot groups measured in Kodaikanal Observatory (KOB) and the amplitude of the solar cycle (see [Javaraiah 2023](#)). Here also no significant correlation is found between the slope of Joy's law determined from the KOB tilt-angle data and the residual covariance. However, we have used the KOB sunspot data that are available at the website www.ngdc.noaa.gov/stp/solar/sunspotregionsdata.html. The aforementioned results need to be verified by using the data of the digitized white-light images of KOB ([Ravindra et al. 2021](#)). [Tlatova et al. \(2018\)](#) have studied Joy's law by using the digitized sunspot drawings from Mount Wilson Observatory in Solar Cycles 15–24 and found no significant correlation between the mean tilt angle and the amplitude of a solar cycle. Here we also determined the coefficients of Joy's law from the mean values of the tilt angles in different 10° latitude intervals (having 5° overlaps) given in Table 2 of [Tlatova et al. \(2018\)](#) for each of Solar Cycles 15–24. In this case also no significant correlation is found between the slope of Joy's law and the coefficient of angular momentum transport. This implies there exists a kind of uniqueness in the MWOB tilt angle dataset that were used here compared to the right now available other tilt angle datasets.

ACKNOWLEDGEMENTS

The author thanks the anonymous referee for useful comments and suggestions. He thanks Manjunath Hegde for fruitful discussion. He acknowledges the work of all the people who contribute to and maintain the GPR, DPD, MWOB and KOB sunspot databases. He used the maximum and minimum epochs of Solar Cycles 12–24 determined by [Pesnell \(2018\)](#) from the time series of 13-month smoothed monthly mean values of version 2 of international sunspot number (SN) available at www.sidc.be/silso/datafiles. The Sun's internal rotation rates derived from the GONG measurements during 1995–2009 was provided by H. M. Antia.

DATA AVAILABILITY

All data generated or analysed during this study are included in this article.

REFERENCES

- Baranyi T., 2015, *MNRAS*, 447, 1857
 Baranyi T., Győri L., Ludmány A., 2016, *Sol. Phys.*, 291, 3081
 Brun A. S., 2004, *Sol. Phys.*, 220, 333
 D'Silva S., Choudhuri A. R., 1993, *A&A*, 272, 621
 Fisher G. H., Fan Y., Howard R. F., 1995, *ApJ*, 438, 463
 Gao P.-X., 2023, *Sol. Phys.*, 298, 21
 Gilman P. A., 1986, In: [Sturrock P.A., et al. \(eds.\), Physics of the Sun, \(Dordrecht: D. Reidel\)](#), 1, 95
 Győri L., Ludmány A., Baranyi T., 2017, *MNRAS*, 465, 1259
 Hale G. E., Ellerman F., Nicholson S. B., Joy A. H., 1919, *ApJ*, 49, 153
 Hanasoge S. M., 2022, *Living Rev. Sol. Phys.*, 19, 3
 Howard R. F., 1991, *Sol. Phys.*, 136, 251

- Howard R. F., 1996a, *ARA&A*, 34, 75
 Howard R. F., 1996b, *Sol. Phys.*, 167, 95
 Howard R. F., 1996c, *Sol. Phys.*, 169, 293
 Javaraiah J., 2013, *Sol. Phys.*, 287, 197
 Javaraiah J., 2021, *Sol. Phys.*, 296, 152
 Javaraiah J., 2023, *Sol. Phys.*, 298, 106
 Javaraiah J., Komm R. W., 1999, *Sol. Phys.*, 184, 41
 Javaraiah J., Ulrich R. K., 2006, *Sol. Phys.*, 237, 245
 Jiao Q., Jiang J., Wang Z.-F., 2021, *A&A*, 653, 27
 Kutsenko A. S., Abramenko V. I., 2021, *Open Astron.*, 30, 219
 Pesnell W. D., 2018, *Space Weather*, 16, 1997
 Petrovay K., Christensen U. R., 2010, *Space Sci. Rev.*, 155, 371
 Poljančič I., et al., 2011, *Cent. Eur. Astrophys. Bull.*, 35, 59
 Ravindra B., Chowdhury P., Javaraiah J., 2021, *Sol. Phys.*, 296, 2
 Snodgrass H. B., Dailey S. B., 1996, *Sol. Phys.*, 163, 21
 Sudar D., Skokić I., Ruždjak D., Brajša R., Wöhl H., 2014, *MNRAS*, 439, 2377
 Sudar D., Brajša R., Skokić I., Poljančič Beljan I., Wöhl H., 2017, *Sol. Phys.*, 292, 86
 Tlatova K., et al., 2018, *Sol. Phys.*, 293, 118
 Ward F., 1965, *ApJ*, 141, 534
 Zhao J., Kosovichev A. G., 2004, *ApJ*, 603, 776

This paper has been typeset from a $\text{\TeX}/\text{\LaTeX}$ file prepared by the author.